Electron Exchange between Fe(II)-Horse Spleen Ferritin and Co(III)/Mn(III) Reconstituted Horse Spleen and *Azotobacter vinelandii* Ferritins†

Bo Zhang,‡ John N. Harb,§ Robert C. Davis,|| Sang Choi,⊥ Jae-Woo Kim,⊥ Tim Miller,§ Sang-Hyon Chu,⊥ and Gerald D. Watt*,‡

Departments of Chemistry and Biochemistry, Chemical Engineering, and Physics, Brigham Young University, Provo, Utah 84602, and NASA Langley Research Center, Hampton, Virginia 23681

Received January 25, 2006; Revised Manuscript Received March 17, 2006

ABSTRACT: *Azotobacter vinelandii* bacterioferritin (AvBF) containing 800−1500 Co or Mn atoms as Co(III) and Mn(III) oxyhydroxide cores (Co-AvBF, Mn-AvBF) was synthesized by the same procedure used previously for horse spleen ferritin (HoSF). The kinetics of reduction of Co-AvBF and Mn-AvBF by ascorbic acid are first-order in each reactant. The rate constant for the reduction of Mn-AvBF (8.52 M^{-1} min^{-1}) is ∼12 times larger than that for Co-AvBF (0.72 M^{-1} min^{-1}), which is consistent with a previous observation that Mn-HoSF is reduced ∼10-fold faster than Co-HoSF [Zhang, B. et al. (2005) *Inorg. Chem. 44*, 3738−3745]. The rates of reduction of M-AvBF (M = Co and Mn) are more than twice that for the reduction of the corresponding M-HoSF. HoSF containing reduced Fe(II) cores (Fe(II)-HoSF), prepared by methyl viologen and CO, also reduces M-HoSF and M-AvBF species, with both cores remaining within ferritin, suggesting that electrons transfer through the ferritin shell. Electron transfer from Fe(II)-HoSF to Co-AvBF occurs at a rate ∼3 times faster than that to Co-HoSF, indicating that the Co cores in AvBF are more accessible to reduction than the Co cores in HoSF. The presence of nonconductive (SiO_2) or conductive (gold) surfaces known to bind ferritins enhances the rate of electron transfer. A more than ∼4-fold increase in the apparent reaction rate is observed in the presence of gold. Although both surfaces (SiO_2 and gold) enhance reaction by providing binding sites for molecular interaction, results show that ferritins with different mineral cores bound to a gold surface transfer electrons through the gold substrate so that direct contact of the reacting molecules is not required.

Ferritins are naturally occurring iron storage proteins that contain up to 4500 Fe atoms as Fe(O)OH within their hollow 8.0 nm spherical protein interiors (*1*, *2*). Most ferritins from plants, animals, and bacteria share a common structure consisting of 24 similar subunits arranged in 432 symmetry to form two-, three-, and four-fold symmetry axes. A recently identified ferritin-like DNA protection protein isolated from *Listeria innocua* is, however, composed of 12 identical 18 kDa subunits, which self-assemble into an empty cage having 23 symmetry (*3*). Hydrophilic channels that are ∼0.4 nm in diameter penetrate the protein shell along the three-fold symmetry axes and are considered the pathways for Fe(II) entry during iron deposition. The mineral core of ferritins is easily removed by reduction and chelation to form apo ferritin, and new mineral cores can be reconstituted by addition of M^{2+} in the presence of an oxidant, which is usually O_2.

Since the first synthesis of inorganic nanophase materials in this supramolecular protein cage (*4*), there has been great interest in the fabrication of nanoparticles by taking advantage of the "nano-reactor" activity of the inner cavity of ferritin for biomineralization. These new ferritin mineral cores range from Co (*5*), Mn (*6*, *7*), magnetite (*8*), Ni, and Cr nanoparticles (*9*), all resembling native ferritin cores, to mineral cores containing technologically interesting materials such as CdS (*10*).

Earlier studies showed that, in the absence of chelators at pH > 7.0, the oxy-hydroxide cores of animal ferritins and the phospho-hydroxide mineral cores of bacterioferritins undergo rapid reversible reduction at potentials of −250 to −420 mV/NHE to produce stable Fe(II) cores with all iron atoms remaining within the ferritin interior (*11*). An important aspect of core reduction is how electrons enter and leave the mineral cores through the 2.0 nm protein shell, and two mechanisms have been proposed. These are (1) diffusion of small redox reagents (<0.40 ∼ 0.60 nm) into the ferritin interior via the three-fold channels with direct reaction at the mineral surface and (2) electron transfer through the protein shell.

Various studies have evaluated the rates of entry of small molecules into the ferritin interior via the protein pores and suggest this process is slow, occurring over tens of minutes, and is highly dependent on the size and charge of the diffusant (*12*−*15*). It seems unlikely then, that large reductants enter the channels to directly and rapidly reduce the mineral cores (*11*, *16*). This conclusion is consistent with

† This work was supported by the National Aeronautics and Space Administration (NASA) Grant NCC-1-02005.

* To whom correspondence should be addressed. Phone, 801-422-4561; fax, 801-422-5474; e-mail, gdwatt@chem.byu.edu.

‡ Department of Chemistry and Biochemistry, Brigham Young University.

§ Department of Chemical Engineering, Brigham Young University.

|| Department of Physics, Brigham Young University.

⊥ NASA Langley Research Center.

10.1021/bi060164d CCC: $33.50
Published on Web 04/12/2006

experiments where reductants too large to enter the channels were found to rapidly reduce the mineral core, suggesting that electron transport pathways extend through the protein shell (*11*). Redox centers were reported in animal ferritins that might mediate such transfers (*16*). In bacterioferritins, 12 heme groups are located on the inner surface of the protein and span about one-half of the protein shell (*17*). It was proposed that these heme groups facilitate the electron transfer (ET)[1] through the bacterioferritin shell (*16*, *18*, *19*).

In addition to these previous redox studies, recent results show that ferritins absorb on metal electrode surfaces, which provides an alternative method for examining the reduction properties of surface-bound ferritins. Using cyclic voltammetry, Zapien et al. were able to measure the direct electron transfer between ferritin and bare or modified gold electrodes, and well-defined current−potential curves were observed (*20*, *21*). Controlled potential electrolysis measurements indicated that adsorption of ferritins preceded electron transfer and the number of electrons transferred corresponded to the number of iron atoms present in the core. Huang et al. also showed that pig spleen ferritin reacts directly with Pt electrodes and undergoes reversible redox reactions (*22*). More recently, Xu et al. performed electrical conductivity measurements on both single molecules and monolayer films of ferritins on flat gold surfaces using conductive AFM (*23*). These studies indicate that electron transfers through the ferritin shell, and that the mineral core enhances the electronic conductivity of the protein.

In a previous paper, we reported the rate of reduction and the reduction potentials of HoSF containing Co(III) or Mn(III) oxyhydroxide mineral cores and showed that the mildly oxidizing Co and Mn cores could be reduced to form stable Co(II) and Mn(II) cores retained within the ferritin interiors (*24*). The ability to make ferritins with both oxidizing and reducing mineral cores presents an opportunity to evaluate electron exchange between ferritins containing mineral cores with different redox states. Such studies may provide insights into how electrons are exchanged from the mineral core through the protein shell to external redox agents during the physiological functions of iron storage and release.

In this paper, we report measurements of the kinetics of reduction of *Azotobacter vinelandii* bacterioferritin (AvBF) containing Co or Mn mineral cores using two reductants, ascorbic acid and Fe(II)-HoSF. The measured rates were compared to rates from similar experiments performed with the HoSF analogues. The influence of gold and SiO_2 surfaces on the reaction rates was also examined. The present work has shown, for the first time, that ferritins containing oxidizing or reducing cores can serve as electron acceptors or donors, and exchange their electrons through the protein shell by direct contact when free in solution or at a faster rate when bound to either a nonconducting or a conducting surface.

[1] Abbreviations: HoSF, horse spleen ferritin; AvBF, *A. vinelandii* bacterioferritin; M-HoSF or M-AvBF, ferritin with Co(III), or Mn(III) oxyhydroxide core; M(II)-HoSF or M(II)-AvBF, ferritin with Co(II), or Mn(II) hydroxide core; MV_r, reduced methyl viologen; AH_2, ascorbic acid; ophen, *o*-phenanthroline; ET, electron transfer; PRC, protein redox center.

MATERIALS AND METHODS

Holo horse spleen ferritin (HoSF) was obtained from Sigma, and iron was removed by the thioglycollic acid procedure (*25*), followed by reaction with dithionite in the presence of bipyridine. Twice crystallized holo and apo *Azotobacter vinelandii* bacterioferritins (AvBF) with 12 hemes per 24-mer were isolated and characterized as previously described (*16*). HoSF with Co(III) and Mn(III) oxyhydroxide cores, Co-HoSF and Mn-HoSF, respectively, were prepared at pH 9.0 as previously described (*5*, *6*, *24*). AvBF with Co(III) and Mn(III) oxyhydroxide cores, Co-AvBF and Mn-AvBF, respectively, were prepared by the same procedures. Protein concentrations were determined using the Lowry method and confirmed by the absorbance at 280 nm ($\epsilon = 470\,000\ M^{-1}\ cm^{-1}$) for the apo HoSF 24-mer (*26*). The metal content in the ferritin core was determined by Inductively Coupled Plasma (ICP) atomic emission spectroscopy (Optima 2000).

Kinetics of M-AvBF Reduction by Ascorbic Acid. The kinetics of Co-AvBF reduction by ascorbic acid (AH_2) were monitored at 350 nm by an HP-8453 UV−visible spectrometer. The AH_2 concentration was kept in excess and thus was essentially constant throughout the course of an experiment. Aliquots of Co-AvBF ([Co] = 1.59 mM, [AvBF] = 1.26 μM, ~1210 Co/AvBF) were added to 1 mL of MOPS buffer (0.025 M at pH 9.0 with 0.05 M NaCl), and the optical spectra were taken to determine the extinction coefficient of Co(III)-AvBF at 350 nm. Then, excess AH_2 (100 μL, 5 mM) was added, and the decreasing absorbance at 350 nm was recorded as a function of time. The final absorbance at 350 nm was due to Co(II)-HoSF, the concentration of which was verified by coulometry as described previously (*24*).

The kinetics of Mn-AvBF reduction by AH_2 were determined both on a stopped-flow kinetic instrument (Applied Photophysics, U.K.) and with the flow-cell system described previously (*27*). Similar results were obtained from both methods. In the flow-cell measurement, aliquots of Mn-AvBF ([Mn] = 3.09 mM, [AvBF] = 2.56 μM, ~1200 Mn/AvBF) were diluted to 2 mL with MOPS or AMPSO buffer, pH 9.0. The spectra were taken, and then 100 μL of AH_2 (5 mM) was added. The absorbance change at 450 nm, the wavelength where Mn(O)OH absorbs, was recorded against time.

Reduced Fe(II) Core of HoSF. HoSF containing a reduced iron core (Fe(II)-HoSF) was prepared at pH 8.0−9.0 by reduction of holo HoSF with reduced methyl viologen (MV_r) in a Vacuum Atmospheres glovebox at oxygen concentrations <0.1 ppm (Nyad O_2 Monitor). Electron exchange reactions between various ferritins were also conducted under these anaerobic conditions to prevent inadvertent oxidation by O_2. Fe(II)-HoSF prepared by low potential chemical reductants is susceptible to Fe^{2+} loss by chelation; thus, the nonchelating MV_r reductant was used to minimize Fe^{2+} loss (*28*). Generally, 1.0 mL of holo HoSF ([HoSF] = 0.1 mM, [Fe] = 0.18 M) in 25 mM MOPS and 50 mM NaCl, pH 8.0, containing 0.1−0.5 mM MV_o was made anaerobic, and 0.1 μM CO dehydrogenase (*29*, *30*) (CODH from *Rhodosprillium rubrum*, was obtained from Dr. Richard Watt at the University of New Mexico) was added at 1.0 atm of CO. The intense blue color of MV_r rapidly formed, and the reaction was allowed to continue for 30 min, during which

Fe(II)-HoSF was formed as outlined by reactions 1−4.

$$CO + H_2O \xrightarrow{CODH} CO_2 + 2e^- + 2H^+ \quad (1)$$

$$2MV_o + 2e^- \rightarrow 2MV_r \quad (2)$$

$$2MV_r + 2Fe(O)OH + 2H_2O \rightarrow 2Fe(OH)_2 + 2MV_o + 2OH^- \quad (3)$$

$$CO + 2Fe(O)OH + H_2O \rightarrow CO_2 + 2Fe(OH)_2 \quad (4)$$

The residual MV_r and/or any unstable Fe(II) were removed by cation-exchange chromatography using an anaerobic 0.5 cm × 3.0 cm column of Dowex 50W-X8 cation-exchange resin (J. T. Baker). The Fe^{2+} content in this newly formed, nearly colorless Fe(II)-HoSF was measured optically by reaction with *o*-phenanthroline ($\epsilon_{511\ nm} = 9640\ cm^{-1}\ M^{-1}$) or 2,2′-bipyridine ($\epsilon_{520\ nm} = 8400\ cm^{-1}\ M^{-1}$) and confirmed by ICP.

Electron Exchange between Ferritins Free in Solution. The kinetics of Co-HoSF and Co-AvBF reduction by Fe(II)-HoSF were determined at pH 9.0 by measuring the rate of Fe^{2+} decrease as Fe(II)-HoSF transfers electrons to the Co(III) cores in the other ferritin. Direct monitoring of the absorbance of Co cores is not possible because of the formation of the interfering Fe(III) core. Fe(II)-HoSF containing ∼1500 Fe ([Fe(II)] = 0.76 mM, [HoSF] = 0.51 μM) and Co-HoSF ([Co] = 3.51 mM, [HoSF] = 2.91 μM) or Co-AvBF ([Co] = 1.59 mM, [AvBF] = 1.26 μM) containing 800−1300 metal atoms were added anaerobically at a 1:1 ratio of metal ions to 1 mL of degassed MOPS (25 mM, pH 9.0, and 50 mM NaCl). At ∼30 s intervals, 0.2 mL of the mixed solutions was transferred to separate vials containing excess ophen or bipyridine in 0.8 mL of buffer. The amount of $[Fe(ophen)_3]^{2+}$ or $[Fe(bipy)_3]^{2+}$ that formed established the amount of unreacted Fe(II) that had not undergone electron transfer. The reaction was also conducted at pH 7.5 to evaluate the effect of OH^- concentration on the rate of ET.

As a control, similar experiments were conducted anaerobically in a dialysis cell with Fe(II)-HoSF or Co-AvBF separated by a 10 kDa MW cutoff dialysis membrane. About 1.5 mL of each ferritin solution was placed in separate compartments of the dialysis cell and stirred. Then 100 μL aliquots were removed from the Fe(II)-HoSF side and reacted with excess ophen over a period of >2 h. During this interval, no loss of Fe^{2+} occurred. All of the electron exchange experiments were repeated with ferritins containing similar but slightly different-sized mineral cores, and similar results were obtained.

Electron Exchange on a Gold or SiO_2 Surface. The effect of a gold surface on the ET process was evaluated by putting a clean gold foil (∼1.8 cm^2) into the MOPS buffer (25 mM, pH 9.0, and 50 mM NaCl) followed by simultaneous addition of Fe(II)-HoSF and Co-HoSF or Co-AvBF at the same concentrations as above. The gold foil was originally cleaned in "Piranha" solution (a mixture of 7 parts of H_2SO_4 and 3 parts of H_2O_2) and thoroughly rinsed with MilliQ water. The cleanliness of gold surfaces was checked by atomic force microscopy (AFM). The solution was stirred, and the progress of the reaction was recorded optically with ophen as described above. Similar electron exchange experiments were conducted with SiO_2, Pyrex, and polypropylene surfaces to determine how these surfaces affected the rate of ET between various ferritins.

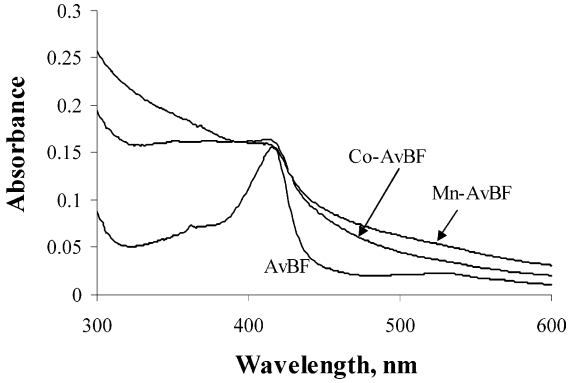

FIGURE 1: Optical spectra of 0.06 μM AvBF, Co-AvBF (0.072 mM Co, [AvBF] = 0.058 μM) and Mn-AvBF (0.075 mM Mn, [AvBF] = 0.062 μM). The absorption at 417 nm is due to the oxidized heme group, but otherwise, the spectra are similar to those of Co-HoSF and Mn-HoSF (*24*).

To further establish the role of gold as the ET pathway, the same dialysis cell with Fe(II)-HoSF and Co-HoSF separated by a membrane was employed except that two gold electrodes were inserted in the Fe(II)-HoSF and Co-HoSF solutions (both at pH 8), respectively, through a hole in the wall of the dialysis cell. The two gold electrodes were then connected to a high-impedance voltammeter, and the cell voltage was recorded. The two electrical leads were next connected directly to short-circuit the "bulk cell" or through a Load Measurement Box (Heliocentris Energie System) to measure the potential difference between Fe(II)-HoSF and Co-HoSF and to control the rate of cell discharge. The Fe(II) concentration in the Fe(II)-HoSF compartment was measured optically using ophen during cell discharge to correlate current flow with conversion of Fe(II)-HoSF to Fe(III)-HoSF.

RESULTS

The formation of Co or Mn cores within AvBF occurred at about the same rates as in HoSF and produced similarly sized cores. Extensive protein precipitation occurred when the formation of mineral cores containing >2000 metal atoms was attempted. The mineral cores were stable for months when maintained at pH values greater than 8.0. Similar optical spectra were obtained for the HoSF (*24*) and AvBF mineral cores, except that Co- and Mn-AvBF had the oxidized heme Soret spectrum (*31*) superimposed (∼420 nm), as shown in Figure 1. This result suggests that the Co and Mn cores formed in these two different ferritin species are similar (*32*).

We reported previously that both Co-HoSF and Mn-HoSF could be reduced by a variety of reducing agents, and that the reduction of Co-HoSF was 10-fold slower than that of Mn-HoSF when ascorbic acid was used as the reductant (*24*). In both cases, the M(II) cores in HoSF interior were stable for long periods. The present study compares the behavior of bacterioferritins containing similar mineral cores with that previously observed for HoSF.

Co-AvBF and Mn-AvBF Reduction by AH_2. Figure 2 shows a series of measurements for the reduction of Co-AvBF by AH_2 as a function of Co concentration at pH 9.0.

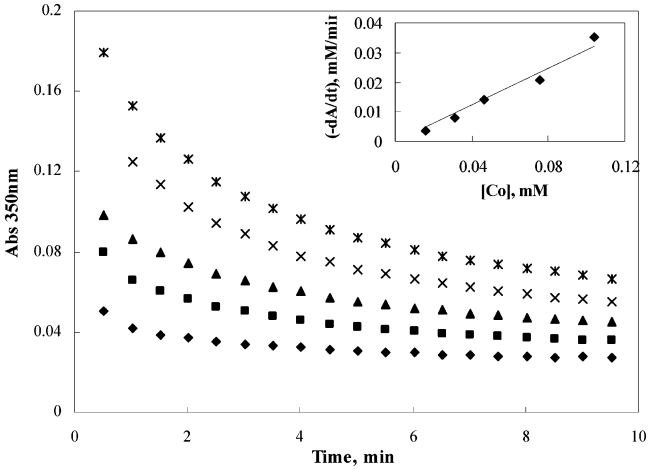

FIGURE 2: Kinetics of Co-AvBF ([Co] = 1.59 mM, [AvBF] = 1.26 μM, ~1210 Co/AvBF) reduction by ascorbic acid (100 μL, 5.0 mM) in 1.0 mL 0.025 M MOPS, and 0.05 M NaCl, pH 9.0. The Co concentration of Co-AvBF was from bottom to top: 0.016, 0.031, 0.046, 0.076, and 0.104 mM. Inset: Initial rate was plotted as a function of Co concentration.

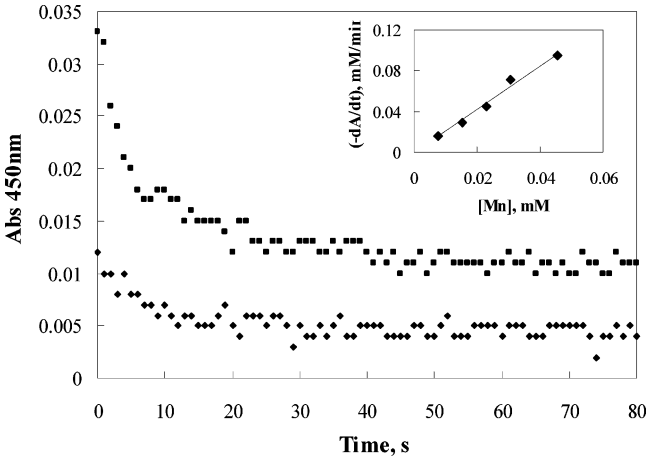

FIGURE 3: Kinetics of Mn-AvBF ([Mn] = 3.09 mM, [AvBF] = 2.56 μM, ~1200 Mn/AvBF) reduction by ascorbic acid (100 μL, 5.0 mM) at 0.008, 0.015, 0.023, 0.031, and 0.046 mM Mn-AvBF in 2.0 mL 0.025 M MOPS and 0.05 M NaCl, pH 9.0. Only the kinetic curves at the first and fourth concentration of Mn-AvBF were shown, and the others were omitted for clarity. Inset: Initial rate was plotted as a function of Mn concentration.

The reaction is typically completed within 10 min. A plot of the initial rate as a function of the Co concentration with a 10-fold excess of AH_2 gives a straight line as shown in the inset, indicating that the reaction is first-order in Co-AvBF. When a constant and excess amount of Co-AvBF was reacted with increasing amounts of AH_2, a similar linear plot was observed (data not shown), indicating a first-order reaction in ascorbic acid. An overall second-order rate constant of 0.72 M^{-1} min^{-1} was determined and is about 1.5 times faster than that of 0.53 M^{-1} min^{-1} for the reduction of Co-HoSF (*24*). The molar absorptivities of the Co(III) and Co(II) cores in AvBF at 350 nm were determined to be 1761 ± 90 and 821 ± 40 M^{-1} cm^{-1}, respectively, and are similar to those of the respective cores in HoSF, indicating that similar cores are formed in both ferritins. The reaction of Mn-AvBF with excess but constant AH_2 is shown in Figure 3 and is much faster than that of Co-AvBF. The reaction was also first-order in both Mn-AvBF and AH_2. The molar absorbances of the Mn(III) and Mn(II) cores in AvBF

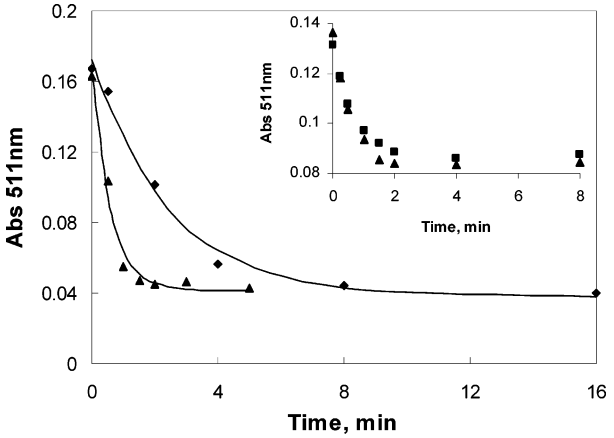

FIGURE 4: Electron exchange between Fe(II)-HoSF and Co-HoSF in MOPS (pH 9) in the absence (♦) and presence (▲) of a gold foil (~1.8 cm^2), as monitored by the decreasing concentration of Fe(II) using ophen. The solid lines are single-exponential fits. The conditions are as follows: Fe(II)-HoSF (0.086 mM Fe^{2+}, 0.058 μM HoSF, final concentrations), Co-HoSF (0.086 mM Co, 0.070 μM HoSF), in 1.2 mL 0.025 M MOPS and 0.05 M NaCl, pH 9. A total of 200 μL of solution was taken out each time to 0.8 mL of ophen in MOPS, and absorbance at 511 nm was recorded. Inset: Same as Figure 4, but in the presence of a 2.3 cm^2 gold (▲) or 3.8 cm^2 SiO_2 surface (■). Curve fitting shows the rate constants for electron exchange are 1.87 and 1.56 min^{-1} with gold and SiO_2, respectively.

at 450 nm were 747 ± 26 and 248 ± 16 M^{-1} cm^{-1}, respectively, and are similar to those for the respective cores in HoSF. The second-order rate constant of 8.52 M^{-1} min^{-1} for Mn-AvBF was about twice of Mn-HoSF and ~12-fold faster than that of Co-AvBF. This result is consistent with previous observations that the reduction of Mn-HoSF was ~10-fold faster than that of Co-HoSF using AH_2 as the reductant (*24*). Because the protein shell is constant in both Co-HoSF and Mn-HoSF, and different but constant in Co-AvBF and Mn-AvBF, the ~10−12-fold increase in rate for the reduction of Mn(III) cores relative to the Co(III) cores must reflect differences in the reducibility of the cores themselves.

Comparison of the reduction rate of Co-HoSF and Co-AvBF or Mn-HoSF and Mn-AvBF by AH_2 shows that the reduction of similar mineral cores is 1.5−2.0 times faster with AvBF than HoSF. Possible explanations for this behavior are discussed later.

Electron Exchange between Fe(II)-HoSF and M-HoSF. Having established that Co- and Mn-AvBF are easily synthesized and are reduced by AH_2 at rates ~2-fold faster than their corresponding HoSF analogues, we sought to evaluate their reducibilities by Fe(II)-HoSF and compare them to those of Co- and Mn-HoSF. Such a comparison with the common and large electron source, Fe(II)-HoSF, should also provide additional insights into the electron transfer (ET) process through the ferritin protein shells.

When the procedure described above was used, Fe(II)-HoSF was readily formed with greater ease and reproducibility than the methods used previously (*11*, *16*). The rate of Fe^{2+} release from Fe(II)-HoSF by bipyridine or ophen was much faster than the rate of electron exchange, allowing the reaction to be followed by measuring the Fe^{2+} concentration remaining in Fe(II)-HoSF as a function of time.

The upper curve in Figure 4 shows that, when Fe(II)-HoSF and Co-HoSF were mixed at pH 9.0, the amount of Fe^{2+}

Scheme 1: Electron Transfer Is Proposed to Occur from the Fe^{2+} Mineral Core of HoSF to the Co^{3+}/Mn^{3+} Mineral Core of HoSF or AvBF through the Respective Protein Shells

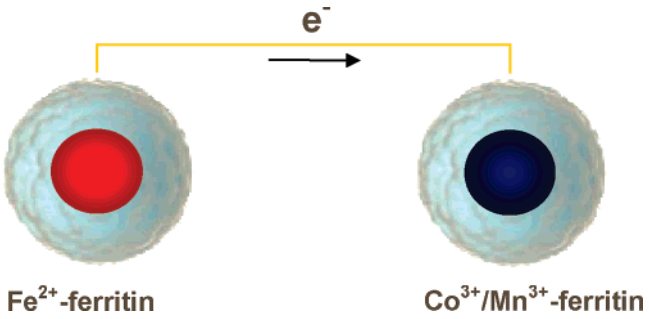

present in Fe(II)-HoSF decreased to near zero within 4 min. Reaction 7 summarizes the overall electron exchange reaction, and Scheme 1 is a schematic view of the process. Although reaction 7 shows no overall OH^- exchange and would appear to be independent of pH, it can be viewed conceptually as the sum of reaction 5, which takes up one OH^-, and reaction 6, which releases an OH^-. Therefore, it is possible that the overall rate may be influenced by pH.

$$\text{Fe(II)-HoSF} + OH^- = \text{Fe-HoSF} + H_2O + e \quad (5)$$

$$\text{Co-HoSF} + H_2O + e = \text{Co(II)-HoSF} + OH^- \quad (6)$$

$$\text{Fe(II)-HoSF} + \text{Co-HoSF} = \text{Fe-HoSF} + \text{Co(II)-HoSF} \quad (7)$$

However, when reaction 7 was run at pH 7.5, no change was seen, indicating that over this pH range the ~15-fold change in OH^- concentration does not alter the rate. Because the M(II)-HoSF (M = Fe, Co, and Mn) species are not stable below pH 7.0 and the protein denatures above pH 10.0, further evaluation of the pH effect was not performed.

Although Fe(II)-HoSF is stable at pH 8.0 with respect to $Fe(OH)_2 = Fe^{2+} + 2OH^-$, the possibility exists that some Fe^{2+} ions dissociate from Fe(II)-HoSF and rapidly migrate through the solution into the Co-HoSF cavity to reduce the Co core, forming an $Fe(OH)_3$ precipitate (*24*). However, this possibility was ruled out because, at the conclusion of the experiment, the solution was centrifuged and no precipitate was observed.

To further eliminate the possibility of Fe^{2+} transfer, Fe(II)-HoSF and Co-HoSF or Co-AvBF were placed in two compartments of a dialysis cell separated by a 10 kDa membrane, through which small ions such as Fe^{2+} and OH^- can transfer but not the ferritin molecules. Thus, free Fe^{2+} released from Fe(II)-HoSF would be able to move across the membrane, while the iron associated with the ferritin would not. Analysis showed that no iron transfer from the Fe(II)-HoSF compartment to the Co-HoSF compartment occurred over a 2-h period (Figure 5, upper curve). Similar results were obtained when Fe(II)-HoSF and Co-AvBF were separated in the same way. These results established that, when ferritins with Fe(II) and Co(III) cores were separated by a dialysis membrane, no electron exchange occurred and no free Fe^{2+} was transferred. For electron exchange to occur, direct contact of these two ferritin species is required when both are free in solution.

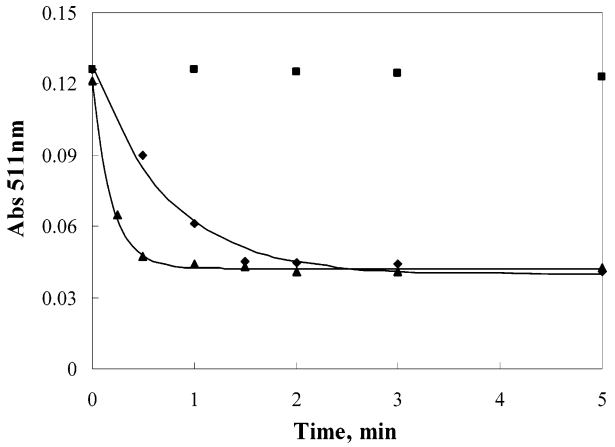

FIGURE 5: Electron exchange between Fe(II)-HoSF and Co-AvBF in MOPS (pH 9.0) separated by a membrane (■), in the absence (♦) and presence (▲) of a gold foil (~1.8 cm^2), as monitored by the decreasing concentration of Fe(II) using ophen. The solid lines are single-exponential fits. The conditions are as follows: Fe(II)-HoSF (0.065 mM Fe^{2+}, 0.045 μM HoSF, final concentrations), Co-AvBF (0.066 mM Co, 0.052 μM AvBF), in 1.2 mL 0.025 M MOPS, and 0.05 M NaCl, pH 9. A total of 200 μL of solution was taken out each time to 0.8 mL of ophen in MOPS, and absorbance at 511 nm was recorded. Curve fitting shows the rate constants for electron exchange are 1.46 and 5.30 min^{-1} in the absence or presence of gold surface, respectively, while no Fe(II) decrease was observed over 2 h when Fe(II)-HoSF and Co-AvBF were separated by a dialysis membrane.

Using the same dialysis cell, we conducted another important experiment. A gold electrode was placed in each compartment and then connected to a high-impedance voltammeter. A stable (>30 min) voltage of 0.45 V was measured, which is equivalent to the voltage of 0.41 ± 0.05 V predicted from the measured Co(III)-HoSF and Fe(II)-HoSF half cells (*24*). Similarly, a voltage of 0.35 V was measured when Mn(III)-HoSF and Fe(II)-HoSF were placed in the two compartments and connected through a gold electrode. When the cell was short-circuited, current flowed through the circuit and the Fe(II) content of Fe(II)-HoSF decreased by 80% in ~1.0 min, indicating that ET occurred between the ferritin molecules on opposite sides of the membrane and ferritin was in electrical contact with the electrode. At the end of the experiment, the current flow was 0, and Co(II)-HoSF and Fe(III)-HoSF were formed. Since no Fe^{2+} was transferred, the only way for electrons to exchange between the separated ferritins was for the two HoSF species to communicate directly with the electrodes and transfer electrons through the gold electrodes.

Electron Exchange between Fe(II)-HoSF and M-AvBF. The top curve in Figure 4 and the middle curve in Figure 5 compare the rate of ET between Fe(II)-HoSF and Co-HoSF (the protein shell is in common) with that between Fe(II)-HoSF and Co-AvBF (different protein shells). The rate with Co-AvBF is ~4-fold faster than that with Co-HoSF, a result consistent with the faster reduction of Co-AvBF by AH_2 relative to Co-HoSF. Electron exchange between Fe(II)-HoSF and Mn-HoSF was also measured using the same procedure, and the reaction was complete in 30 s or less, consistent with the ~10-fold faster reduction rate of Mn-HoSF over that of Co-HoSF, which would correspond to a minimum of 24 s for completion. This result demonstrates that ET through both protein shells is not limiting and is faster than the reduction of the Mn mineral core. It also suggests that (1)

Table 1: First Order Rate Constants from Exponential Fit of the Electron Exchange Reactions between Fe(II)-HoSF and Co-HoSF and -AvBF in the Absence and Presence of a Surface

	Co-HoSF				Co-AvBF	
	− Au	Au (1.8 cm^2)	Au (2.3 cm^2)	SiO_2 (3.8 cm^2)	− Au	Au
k, min^{-1}	0.44 ± 0.03	1.75 ± 0.11	1.87 ± 0.13	1.56 ± 0.10	1.46 ± 0.09	5.30 ± 0.35

the Co mineral core is reduced more slowly than the Mn core when constrained in the same type of ferritin cavity and (2) reduction of the mineral core in AvBF is faster than that of the corresponding core in HoSF, when using Fe(II)-HoSF as reductant.

Presence of a Gold or SiO_2 Surface. Ferritins are known to bind to metal surfaces (*34*, *35*), and electron exchange may occur between the mineral cores and metal surface through the protein shell when a proper voltage is applied (*20*−*23*). The results from the above electrochemical cell confirm the ability of ferritins to transfer electrons directly to metal electrodes, presumably through the protein shell. These results also predict an important role of the surfaces in facilitating ET, which is verified by the lower curve in Figure 4. Upon the addition of a small piece of clean gold (1.8 cm^2), the reaction rate increased >4-fold under otherwise identical conditions. To further evaluate this enhancement of ET, additional experiments were performed with Fe(II)-HoSF and Co-HoSF mixed in the presence of either a gold (2.3 cm^2) or a SiO_2 surface (3.8 cm^2) deposited on Si chips. The results are shown in the inset to Figure 4, and the apparent rate constants of 1.87 and 1.56 min^{-1} for gold and SiO_2, respectively, were obtained by fitting the curves to an exponential function. When normalized to the same surface area, both SiO_2 and gold bind the same amount of Fe(II)-HoSF (4×10^{-4} mM Fe^{2+}/cm^2, calculated from the absorbance decrease upon addition of the SiO_2 or gold surface), corresponding to a monolayer coverage of ferritin. Pyrex and polypropylene surfaces did not appear to bind ferritins and did not enhance ET.

Figure 5 shows that the presence of a gold foil also enhances the rate of ET between Fe(II)-HoSF and Co-AvBF by ∼4-fold (lower curve) relative to the rate observed without gold (middle curve). The enhancement of ET by the gold surface was not quantitatively determined for Fe(II)-HoSF and Mn-HoSF or Mn-AvBF, because the reactions were concluded before analysis could be performed. All of the reaction profiles were fit to an exponential function, and the apparent rate constants are summarized in Table 1.

DISCUSSION

Although some differences in overall amino acid contents and sequences are noted between AvBF and HoSF, and the ferroxidase centers are somewhat different (*2*, *17*), they do not interfere with the convenient formation of the two nonphysiological Co and Mn core types in AvBF (*32*). What is most conspicuous is the presence of 12 heme groups in AvBF and their absence in HoSF, and the presence of 3−4 endogenous protein redox centers (PRCs) involving Trp93 in the H-subunit in HoSF and their absence in AvBF (*11*, *36*, *37*). The role of these two types of redox centers in HoSF and AvBF is not known but has been proposed to be electron-transfer sites that facilitate ET across their respective protein shells (*11*, *37*). Electron transfer across the ferritin shell is an important aspect of ferritin function, and at least two types of reactivity have been envisioned: (1) direct reductant entry into the ferritin interior and (2) ET through the ferritin shell. Evidence for both types of reactivity has been presented (*11*, *38*). Here, we explore the physical processes that accompany redox reactions of mineral cores in both HoSF and AvBF using (1) negatively charged ascorbic acid of nominal size to that of the three-fold channel openings and (2) Fe(II)-HoSF with a reducing mineral core whose overall dimensions are too large to enter the ferritin channels. Experiments using these two types of reductants provide insights into the ET process through the ferritin shell, and the reduction properties of the mineral particles within the ferritin interior.

AH_2 Reduction. The overall rate law for reduction of Co-AvBF and Mn-AvBF with AH_2 is identical to that for reduction of the corresponding HoSF species. It was also found that Co-AvBF was reduced ∼12-fold slower than Mn-AvBF. A similar difference was observed for Co-HoSF relative to Mn-HoSF (*24*). With the same reductant and the same protein shell in common (either AvBF or HoSF), the observed difference in rate must be due to a difference in the reduction rate of the cores themselves, which is attributable, at least in part, to a greater stability of the Co(III) mineral core relative to Mn(III).

The type of ferritin also influenced the rate for a given core. In each case, the M-AvBF species are reduced ∼2 times faster by AH_2 than the corresponding M-HoSF species. This behavior was initially attributed to the different natures of these two protein shells: the permeability or the conductivity. However, the 10−12-folds differences in the reduction rates of Co and Mn mineral cores constrained in a common ferritin cavity suggest that the ferritin shells do not limit the reaction rates. Thus, two possible explanations for this behavior are (1) the nature of the mineral core in bacterioferritin enhances its reactivity and (2) the core in AvBF is connected to the protein shell in a manner that facilitates ET relative to transfer in HoSF. In either case, the results indicate that ET through the protein shell is not the limiting process in the reaction.

Initial results presented contradictory views as to whether molecules of the size of AH_2 could diffuse into the interior and reduce the core directly (*12*, *13*), but recent EPR studies showed that molecules with nominal diameters of 0.7−0.9 nm typical of AH_2 do gain access to the ferritin interior but only slowly (*15*, *33*). Therefore, it is unlikely that AH_2 transfers through the ferritin channel and reduces the Co or Mn cores directly because of two factors: (1) it takes ∼60 min for a nitroxide radical of similar size to AH_2 to penetrate the ferritin shell (*33*), while Figures 2 and 3 show that the reduction of Co and Mn mineral cores in AvBF are reduced in less than 1−8 min, a time much faster than that can be accounted for by diffusion and (2) with a pK_a of 4.1, AH_2 is negatively charged at pH 9.0, and negatively charged groups of this nominal size are completely excluded from the HoSF interior (*33*).

Scheme 2: A Schematic Representation of the Redox Potentials for the Oxidants, Reductants, and Mediators: Heme in AvBF and the Protein Redox Center (PRC) in HoSF at pH 8.0[a]

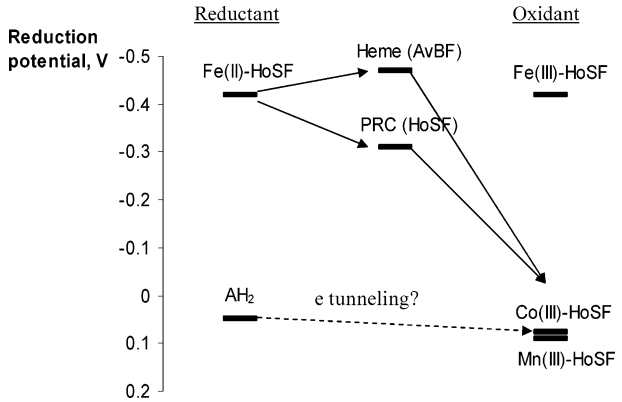

[a] With AH_2 as reductant, the Co and Mn mineral cores in HoSF or AvBF might be reduced by electron tunneling through the 2.0 nm protein shell, the mechanism of which is not known. With Fe(II)-HoSF as reductant, the redox active centers (heme or PRC) mediate the electron transfer.

The ET pathway across the AvBF shell for reduction by AH_2 was initially thought to be due to the presence of the 12 redox-active heme groups partially spanning the AvBF protein. However, the redox potential of AH_2 is +0.05 V at pH 8.0−9.0, while the reduction potential of the heme group in holo AvBF is −0.42 V,[2] making this explanation unlikely. The results indicate that for AH_2 an alternative ET pathway exists in the AvBF shell, which Scheme 2 suggests is electron tunneling. While heme is excluded as a likely endogenous ET agent for AH_2 reduction, it may be functional for reductants with more negative reduction potentials, such as Fe(II)-HoSF.

A similar analysis applied to reduction of Co- and Mn−HoSF mineral cores suggests that the HoSF protein shell also must have an endogenous ET pathway for reduction by AH_2 that is different from the redox center known to be present that operates at −0.31 V (Scheme 2) at pH 8. As with the heme group discussed above, this redox center in HoSF may function with reductants with a more negative reduction potential. The possibility that heme in AvBF and PRC in HoSF conduct ET is next considered.

Electron Transfer from Fe(II)-HoSF to M-HoSF. The large size of Fe(II)-HoSF and the observation that Fe^{2+} remains in the interior of the ferritin suggest that ET must occur directly between Fe(II)-HoSF and Co- and Mn-HoSF through each of the ∼2.0 nm protein shells that isolate the mineral cores. In contrast to reduction by AH_2, ET using the redox center in HoSF is now thermodynamically feasible because Fe(II)-HoSF is a strong reductant at pH 9.0 with an E' value of −0.42 V (*39*). Thus, ET may occur rapidly through the redox centers present in the ferritin shells when Fe(II)-HoSF and Co- or Mn-HoSF encounter each other in solution. It is known that reducing proteins and organic molecules too large to enter the channel openings are capable of rapidly reducing these redox centers in HoSF (*11*, *36*, *39*). Further support comes from the anaerobic addition of Fe^{2+} to HoSF with oxidized PRCs, which produces Fe^{3+} and presumably reduces the redox centers, suggesting the redox centers function in Fe^{2+} oxidation (*40*). Ongoing experiments in our laboratory found that large molecule oxidants, such as cytochrome *c*, are capable of depositing Fe(II) into HoSF, but not as effectively into homopolymers (all heavy or all light chain ferritins) that have no PRCs present (*37*). Taken together, these results indicate that the PRCs in HoSF may act as intermediates (Scheme 2) and subsequently transfer electrons to the mineral cores much faster than electron tunneling as proposed for AH_2.

Electron Transfer from Fe(II)-HoSF to M-AvBF. Comparison of Figure 5 with Figure 4 shows that the rate of Co-AvBF reduction by Fe(II)-HoSF is twice as fast as that observed for Co-HoSF, a result which is consistent with that observed with AH_2. Similarly, this increase in rate could arise from several factors: (1) while apparently identical, the Co mineral cores in HoSF and AvBF could be sufficiently different to affect the kinetics of the mineral core reduction; 2) the mineral cores attach to the protein shell differently, modifying the rate of reduction; and 3) the rate of ET through the AvBF protein shell may be faster than that through the HoSF shell. However, the rapid electron exchange between Fe(II)-HoSF and Mn-AvBF establishes that ET through the ferritin shell is not limiting and thus eliminates possibility 3 above. A previous kinetic study of iron release from AvBF suggested that some iron atoms are associated with the heme groups that limit the reduction rate of the core iron (*18*). Thus, differences in the attachment of the Co or Mn mineral cores to HoSF and AvBF protein shells may explain the differences in rate of ET to the two ferritin species from the common Fe(II)-HoSF reductant. Although Co and Mn oxyhydroxides are nonphysiological mineral cores, the lower accessibility of these cores in HoSF to external reductants relative to AvBF could suggest a better protection of iron to environmental change by the higher organisms.

Effect of Gold and SiO_2 Surfaces. Ferritins adsorb to clean gold surfaces or gold electrodes modified by self-assembled monolayers and exchange electrons with these metal electrodes (*20*−*23*). Figures 4 and 5 show a nearly 4-fold increase in rate upon addition of a small piece of gold to the ferritin-containing solutions. The gold surface may enhance the rate in at least two ways. First, the presence of the surface increases the collision frequency between the two ferritin types. We refer to this possibility as "surface enhancement". The second possibility is that the gold conductor provides an ET pathway so that it is not necessary for the ferritin molecules to contact one another but only contact the gold surface to exchange electrons. This second possibility is considered "conduction enhancement".

To distinguish which of these mechanisms function, the reactions were run in the presence of an insulating SiO_2 surface that also binds ferritin (*41*). The SiO_2 surface can only contribute to surface enhancement by providing reaction sites, which may increase the collision frequency of the bound HoSF species or provide lower activation energy for the electron-transfer reaction. The inset in Figure 4 demonstrates surface enhancement by SiO_2. When both gold and SiO_2 surfaces bind the same amount of ferritin per cm^2, the

[2] The heme reduction potential in apo AvBF is −0.23 V, and that quoted for holo AvBF is −0.42 V. The difference was attributed to the heme-mineral core interaction (*16*). We assume here that the Co and Mn mineral cores in AvBF have the same effect as the Fe mineral core and that the heme reduction potential is −0.42 V for Co- and Mn-AvBF.

reaction rates show that SiO_2 is not as efficient as gold in stimulating ET. When normalized to the same surface area, gold was about twice as effective as SiO_2 (0.81 vs 0.41 min^{-1} cm^{-2}), perhaps due to conduction enhancement.

Electron transfer through gold (conduction enhancement) to and from ferritin mineral cores was demonstrated unequivocally in the electrochemical cell experiment described above where gold wires in each compartment were electrically connected. That experiment showed that Fe(II)-HoSF transferred electrons via the gold wire to reduce Co-HoSF at a rate comparable to the lower curve of Figure 4. The observed cell discharge could only occur by conduction enhancement, as the reactants were in separate cell compartments that made direct interaction impossible. Similar behavior was observed for ET from Fe(II)-HoSF to Co-AvBF, except the reaction rate was about 3 times faster both in the presence and absence of gold (compare Figures 4 and 5). Further support comes from the potential measurements for the Fe(II)-HoSF vs Co- or Mn-HoSF cells. Voltages consistent with theoretical predictions were observed in both cases, suggesting that ferritins containing different metals form an electrochemical cell with Fe(II)-HoSF as the cathode and Co- or Mn-HoSF as the anode.

While ET between ferritins with different redox active minerals in the presence of a gold surface is influenced by both surface exchange and conduction exchange, it is clear that only conduction enhancement operates when only one redox partner is in contact with the electrode. A variety of mediators and surface-modified electrodes have been employed to enhance electron exchange between proteins and electrodes (*42*), but ET between ferritins in the present experiments occurred without deliberate mediation. The process likely requires specific interaction of the proteins with the electrodes to facilitate ET, and it is possible that the correct orientation of the redox centers or electron transport pathways present in the ferritin shell plays an important role. Exploring these possibilities is part of our continuing efforts to understand electron transfer in ferritins and in possibly developing nanoscale electroactive materials and devices based on ferritins.

REFERENCES

1. Theil, E. C. (1987) Ferritin structure gene regulation and cellular function in animals plants and microorganisms, *Annu. Rev. Biochem. 56*, 289−316.
2. Harrison, P. M., and Arosio, P. (1996) The ferritins: molecular properties, iron storage function and cellular regulation, *Biochim. Biophys. Acta 1275*, 161−203.
3. Bozzi, M., Mignogna, G., Stefanini, S., Barra, D., Longhi, C., Valenti, P., and Chiancone, E. (1997) A novel non-heme iron-binding ferritin related to the DNA-binding proteins of the Dps family in *Listeria innocua*, *J. Biol. Chem. 272*, 3259−3265.
4. Meldrum, F. C., Wade, V. J., Nimmo, D. L., Heywood, B. R., and Mann, S. (1991) Synthesis of inorganic nanophase materials in supramolecular protein cages, *Nature 349*, 684−687.
5. Douglas, T., and Stark, V. T. (2000) Nanophase cobalt oxyhydroxide mineral synthesized within the protein cage of ferritin, *Inorg. Chem. 39*, 1828−1830.
6. Mackle, P., Charnock, J. M., Garner, C. D., Meldrum, F. C., and Mann, S. (1993) Characterization of the manganese core of reconstituted ferritin by X-ray absorption spectroscopy, *J. Am. Chem. Soc. 115*, 8471−8472.
7. Meldrum, F. C., Douglas, T., Levi, S., Arosio, P., and Mann, S. (1995) Reconstitution of manganese oxide cores in horse spleen and recombinant ferritins, *J. Inorg. Biochem. 58*, 59−68.
8. Meldrum, F. C., Heywood, B. R., and Mann, S. (1992) Magnetoferritin in-vitro synthesis of a novel magnetic protein, *Science (Washington, D.C.) 257*, 522−523.
9. Okuda, M., Iwahori, K., Yamashita, I., and Yoshimura, H. (2003) Fabrication of nickel and chromium nanoparticles using the protein cage of apoferritin, *Biotech. Bioeng. 84*, 187−194.
10. Wong, K. K. W., and Mann, S. (1996) Biomimetic synthesis of cadmium sulfide- ferritin nanocomposites, *Adv. Mater. (Weinheim, Ger.) 8*, 928−932.
11. Watt, G. D., Jacobs, D., and Frankel, R. B. (1988) Redox reactivity of bacterial and mammalian ferritin: is reductant entry into the ferritin interior a necessary step for iron release, *Proc. Natl. Acad. Sci. U.S.A. 85*, 7457−7461.
12. Stuhrmann, H. B., Haas, J., Ibel, K., Koch, M. H. J., and Crichton, R. R. (1976) Low angle neutron scattering of ferritin studied by contrast variation, *J. Mol. Biol. 100*, 399−413.
13. May, M. E., Fish, W. W., Brown, E. B., Aisen, P., and Fielding, J. (1977) The restrictive nature of apoferritin channels as measured by passive diffusion. In *Proteins of Iron Metabolism* (Brown, E. J., Ed.) pp 31−38, Grune & Stratton, New York.
14. Webb, B., Frame, J., Zhao, Z., Lee, M. L., and Watt, G. D. (1994) Molecular entrapment of small molecules within the interior of horse spleen ferritin, *Arch. Biochem. Biophys. 309*, 178−183.
15. Yang, X., and Chasteen, N. D. (1996) Molecular diffusion into horse spleen ferritin: a nitroxide radical spin probe study, *Biophys. J. 71*, 1587−1595.
16. Watt, G. D., Frankel, R. B., Papaefthymiou, G. C., Spartalian, K., and Stiefel, E. I. (1986) Redox properties and Mössbauer spectroscopy of *Azotobacter vinelandii* bacterioferritin, *Biochemistry 25*, 4330−4336.
17. Andrews, S. C. (1998) Iron storage in bacteria, *Adv. Microb. Physiol. 40*, 282−351.
18. Richards, T. D., Pitts, K. R., and Watt, G. D. (1996) A kinetic study of iron release from *Azotobacter vinelandii* bacterial ferritin, *J. Inorg. Biochem. 61*, 1−13.
19. Stiefel, E. I., and Watt, G. D. (1979) *Azotobacter* cytochrome b557.5 is a bacterioferritin, *Nature 279*, 81−83.
20. Martin, T. D., Monheit, S. A., Niichel, R. J., Peterson, S. C., Campbell, C. H., and Zapien, D. C. (1997) Electron transfer of horse spleen ferritin at gold electrodes modified by self-assembled monolayers, *J. Electroanal. Chem. 420*, 279−290.
21. Zapien, D. C., and Johnson, M. A. (2000) Direct electron transfer of ferritin adsorbed at bare gold electrodes, *J. Electroanal. Chem. 494*, 114−120.
22. Huang, H. Q., Lin, Q. M., and Wang, T. L. (2002) Kinetics of iron release from pig spleen ferritin with bare platinum electrode reduction, *Biophys. Chem. 97*, 17−27.
23. Xu, D., Watt, G. D., Harb, J. N., and Davis, R. C. (2005) Electrical conductivity of ferritin proteins by conductive AFM, *Nano Lett. 5*, 571−577.
24. Zhang, B., Harb, J. N., Davis, R. C., Kim, J. W., Chu, S. H., Choi, S., Miller, T., and Watt, G. D. (2005) Kinetic and thermodynamic characterization of the Co(III) and Mn(III) mineral cores formed in horse spleen ferritin, *Inorg. Chem. 44*, 3738−3745.
25. Treffry, A., and Harrison, P. M. (1978) Incorporation and release of inorganic phosphate in horse spleen ferritin, *Biochem. J. 171*, 313−320.
26. Zhao, G., Bou-Abdallah, F., Yang, X., Arosio, P., and Chasteen, N. D. (2001) Is hydrogen peroxide produced during iron(II) oxidation in mammalian apoferritins? *Biochemistry 40*, 10832−10838.
27. Lindsay, S., Brosnahan, D., Lowery, T. J., Jr., Crawford, K., and Watt, G. D. (2003) Kinetic studies of iron deposition in horse spleen ferritin using O_2 as oxidant, *Biochim. Biophys. Acta 1621*, 57−66.
28. Double, K. L., Maywald, M., Schmittel, M., Riederer, P., and Gerlach, M. (1998) In vitro studies of ferritin iron release and neurotoxicity, *J. Neurochem. 70*, 2492−2499.
29. Ensign, S. A., Bonam, D., and Ludden, P. W. (1989) Nickel is required for the transfer of electrons from carbon monoxide to the iron−sulfur center(s) of carbon monoxide dehydrogenase from *Rhodospirillum rubrum*, *Biochemistry 28*, 4968−4973.
30. Stephens, P. J., McKenna, M. C., Ensign, S. A., Bonam, D., and Ludden, P. W. (1989) Identification of a Ni- and Fe-containing cluster in *Rhodospirillum rubrum* carbon monoxide dehydrogenase, *J. Biol. Chem. 264*, 16347−16350.
31. Watt, G. D., McDonald, J. W., Chiu, C. H., and Reddy, K. R. N. (1993) Further characterization of the redox and spectroscopic

properties of *Azotobacter vinelandii* ferritin, *J. Inorg. Biochem. 51*, 745−758.
32. Allen, M., Willits, D., Young, M., and Douglas, T. (2003) Constrained synthesis of cobalt oxide nanomaterials in the 12-subunit protein cage from *Listeria innocua*, *Inorg. Chem. 42*, 6300−6305.
33. Yang, X., Arosio, P., and Chasteen, N. D. (2000) Molecular diffusion into ferritin: pathways, temperature dependence, incubation time, and concentration effects, *Biophys. J. 78*, 2049−2059.
34. Caruso, F., Furlong, D. N., and Kingshott, P. (1997) Characterization of ferritin adsorption onto gold, *J. Colloid Interface Sci. 186*, 129−140.
35. Hook, F., Rodahl, M., Brzezinski, P., and Kasemo, B. (1998) Measurements using the quartz crystal microbalance technique of ferritin monolayers on methyl thiolated gold: dependence of energy dissipation and saturation coverage on salt concentration, *J. Colloid Interface Sci. 208*, 63−67.
36. Watt, R. K., Frankel, R. B., and Watt, G. D. (1992) Redox reactions of apo mammalian ferritin, *Biochemistry 31*, 9673−9679.
37. Johnson, J. L., Norcross, D. C., Arosio, P., Frankel, R. B., and Watt, G. D. (1999) Redox reactivity of animal apoferritins and apoheteropolymers assembled from recombinant and light human chain ferritins, *Biochemistry 38*, 4089−4096.
38. Yang, D., and Nagayama, K. (1995) Permeation of small molecules into the cavity of ferritin as revealed by proton nuclear magnetic resonance relaxation, *Biochem. J. 307*, 253−256.
39. Watt, G. D., Frankel, R. B., and Papaefthymiou, G. C. (1985) Reduction of mammalian ferritin, *Proc. Natl. Acad. Sci. U.S.A. 82*, 3640−3643.
40. Jacobs, D., Watt, G. D., Frankel, R. B., and Papaefthymiou, G. C. (1989) Fe^{2+} binding to apo and holo mammalian ferritin, *Biochemistry 28*, 9216−9221.
41. Nygren, H. (1993) Nonlinear kinetics of ferritin adsorption, *Biophys. J. 65*, 1508−1512.
42. Frew, J. E., and Hill, H. A. O. (1988) Direct and indirect electron transfer between electrodes and redox proteins, *Eur. J. Biochem. 172*, 261−269.

BI060164D